

Nearest neighbor synthesis of CNOT circuits on general quantum architectures

Xinyu Chen, Mingqiang Zhu, Xueyun Cheng, Pengcheng Zhu and Zhijin Guan

Abstract—In recent years, quantum computing has entered the Noisy Intermediate-Scale Quantum (NISQ). However, NISQ devices have inherent limitations in terms of connectivity and hardware noise, necessitating the transformation of quantum logic circuits for correct execution on NISQ chips. The synthesis of CNOT circuits considering physical constraints can transform quantum algorithms into low-level quantum circuits, which can be directly executed on physical chips. In the current trend, quantum chip architectures without Hamiltonian paths are gradually replacing architectures with Hamiltonian paths due to their scalability and low-noise characteristics. To this end, this paper addresses the nearest neighbor synthesis of CNOT circuits in the architecture with and without Hamiltonian paths, aiming to enhance the fidelity of the circuits after execution. Firstly, a key-qubit priority mapping model for the general architecture with and without Hamiltonian paths is proposed. Secondly, the initial mapping is further improved by using tabu search to reduce the number of CNOT gates after circuit synthesis and enhance its fidelity. Finally, the noise-aware CNOT circuit nearest neighbor synthesis algorithm for the general architecture is proposed based on the key-qubit priority mapping model. Experimental results show that the proposed method can enhance the fidelity of the CNOT circuit by about 64.7% on a real quantum computing device, achieving a significant optimization effect. Furthermore, the method can be extended to other circuits, thereby improving the overall performance of quantum computing on NISQ devices.

Index Terms—CNOT circuit synthesis, nearest neighbor (NN) constraint, Hamiltonian path, hardware noise

I. INTRODUCTION

QUANTUM computing is a new computing paradigm that follows the laws of quantum mechanics to perform complex tasks. It can provide exponential speedups over classical algorithms in integer factorization [1], database search [2], quantum many-body simulation [3], *etc.* Moreover, quantum computing has potential applications in cryptography [4], chemistry [5], artificial intelligence [6] and other areas, and thus it is a very active research area. In recent years, quantum computing has entered the era of Noisy Intermediate-Scale Quantum (NISQ), which supports quantum computing with tens to hundreds of qubits. However, NISQ devices are limited in their ability to apply only a few elementary quantum gates due to the presence of noise. Among these gates, the CNOT gate is widely employed in quantum computing as it can be combined with other single quantum gates to construct a

universal gate library [7]. The circuits composed of CNOT gates cannot be executed directly since the nearest neighbor (NN) constraint and error rate of NISQ devices are affected by the physical architecture. Instead, these circuits must be further transformed into a suitable form that can be implemented on actual quantum hardware.

Currently, there are two main methods to obtain a quantum circuit that satisfies the NN constraint. The first method involves inserting SWAP gates in front of quantum gates that do not satisfy the NN constraint after the initial mapping [8–10]. This ensures the connection of non-nearest neighbor gates on physical qubits. Since a SWAP gate can be decomposed into three CNOT gates, this method necessitates the insertion of additional CNOT gates. Consequently, the number of layers of the final circuit increases, raising the probability of errors in the circuit. The other approach focuses on researching the synthesis of quantum circuits directly under NN constraints that satisfy the physical architecture. Quantum circuit synthesis enables the transformation of a matrix representing a quantum algorithm into a quantum circuit supporting a specific library of gates [11–14]. The synthesis method that generates a synthesis containing only CNOT gates is CNOT quantum circuit synthesis. Although CNOT quantum circuit synthesis methods can produce circuits containing a sequence of CNOT gates, the CNOT circuits after synthesis do not necessarily satisfy the NN constraint of the physical architecture and cannot be executed on real quantum computing devices. To address this issue, the CNOT circuit NN synthesis method that transforms the Boolean matrix into a CNOT circuit satisfying the NN constraint of the physical architecture was proposed to solve this problem [15–23].

Several researchers have dedicated their efforts to the synthesis of quantum circuits. In [15], CNOT circuits are represented as Boolean matrixes and a CNOT circuit synthesis algorithm based on Gaussian elimination and LU decomposition is proposed. However, the NN of the control qubits and the target qubits of the CNOT gates are not considered. A linear NN Gaussian elimination method is proposed in [16], which shares a similar structure to the Gaussian elimination method. But the row operations must be performed between adjacent rows, and this method is only applicable to the NN synthesis problem of CNOT circuits in a one-dimensional (1D) structure. In [17] and [18], the NN synthesis method for CNOT circuits in a two-dimensional (2D) structure was proposed, which relies on Steiner trees to determine the NN interaction paths on a 2D grid. A similar strategy is proposed in [19], and they both use Steiner trees to determine the interaction paths that satisfy the NN constraint. In contrast to the traditional

Xinyu Chen, Mingqian Zhu, Xueyun Cheng and Zhijin Guan, School of Information Science and Technology, Nantong University, Nantong 226019, China, E-mail: xinyu_chen@stmail.ntu.edu.cn, zhu_mqiang@163.com, chen.xy@ntu.edu.cn, guan.zj@ntu.edu.cn.

Pengcheng Zhu, Department of Artificial Intelligence, Suqian University, Suqian, 223800, China, E-mail: 17123@sqc.edu.cn

Gaussian elimination, they do not completely rely on the main diagonal elements in the elimination process, but they use the neighboring elements with value 1 in the Steiner tree to achieve the row elimination. In [20], a new algorithm for CNOT circuit synthesis based on corrected sub-decoding is proposed to solve the problem of synthesizing CNOT circuits with fully connected topologies as well as quantum devices with topologically constrained structures. The authors in [21] aim to reduce the effect of noise on CNOT circuit synthesis, and reduce the number of CNOT gates and circuit depth while reducing the errors generated during the synthesis process.

The above studies mainly focus on CNOT circuit synthesis on quantum architecture with Hamiltonian paths. However, with the development of NISQ devices, the architecture without Hamiltonian paths is gradually replacing those with Hamiltonian paths because of its excellent scalability and high fault tolerance. Consequently, the CNOT circuit synthesis methods designed for architectures with Hamiltonian paths cannot be directly applied to architectures without Hamiltonian paths. Various solutions have been proposed to address this challenge. Both [22] and [23] present ROWCOL methods for implementing NN synthesis of CNOT circuits on arbitrary architectures. These methods prioritize the elimination of certain qubits and subsequently disconnect them. This allows finding suboptimal Hamiltonian paths in architectures where no Hamiltonian paths exist. The size of the problem is gradually reduced. Another approach is to use matrix decomposition techniques [24] to represent the quantum algorithm as a quantum circuit. The circuit is then mapped directly onto the physical architecture and the NN of the qubits are implemented using traditional quantum routing methods [25]. While this approach avoids the reliance on Hamiltonian paths, but it requires more resources and time to implement the NN of quantum circuit, and may not lead to optimal solutions. In practical applications, these drawbacks may lead to lower efficiency of quantum computing or even failure to achieve the desired computational tasks.

With fidelity as the goal, we propose a solution for NN synthesis of CNOT circuits on general quantum architectures. The main contributions of this paper are as follows.

- The challenges associated with CNOT quantum circuit synthesis on quantum architectures without Hamiltonian paths are analyzed, and a key-qubit priority mapping model is proposed to solve the problem. Based on this model, the initial mapping of key qubits is further improved by using tabu search to enhance the circuit fidelity after synthesis.
- Based on the initial mapping strategy of key qubits, a NN synthesis of CNOT circuits method is proposed for the general architecture. This method converges the Boolean matrix by layers under the premise of satisfying the NN constraint, and gradually realizes the matrix transformation, thus transforming into a CNOT circuit with lower error rate.
- The above algorithm is tested on IBMQ's quantum computing cloud platform by using real quantum chip architecture as well as simulators. The experiment results demonstrate a significant improvement in the fidelity of

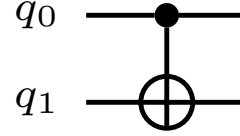


Fig. 1. A CNOT gate.

CNOT quantum circuits on these real quantum computing chip architectures and simulators.

This paper is organized as follows: in Section II, basic concepts involving CNOT circuit synthesis are briefly introduced, such as CNOT circuits, quantum topological constraints and Boolean matrices. In Section III, key qubit-priority mapping for general quantum architectures is implemented, a key qubit-priority model is established, and the key qubit-priority initial mapping is optimized by tabu search. In Section IV, a noise-aware CNOT circuit NN synthesis based on the key qubit-priority model is implemented, and a CNOT circuit NN synthesis algorithm applicable to the general architecture is given. In Section V, the proposed method's optimization of circuit fidelity is verified by the execution results on quantum computing devices. The paper is discussed and summarized in Section VI and VII.

II. BACKGROUND

A. CNOT gate and CNOT circuit

CNOT (Controlled-NOT) gate is a basic two-qubit quantum logic gate that performs a conditional NOT operation on the target qubit depending on the state of the control qubit. Figure 1 shows a graphical representation of a CNOT gate with two input qubits, where q_0 denotes the control bit and q_1 denotes the target bit. The operation of a CNOT gate can be represented by a unitary matrix, which defines the relationship of input and output. The unitary matrix of a CNOT gate is given by Eq. (1).

$$U_{\text{CNOT}} = \begin{bmatrix} 1 & 0 & 0 & 0 \\ 0 & 1 & 0 & 0 \\ 0 & 0 & 0 & 1 \\ 0 & 0 & 1 & 0 \end{bmatrix} \quad (1)$$

This unitary matrix shows that the CNOT gate flips the state of the target qubit if and only if the control qubit is in the $|1\rangle$ state, which can be expressed in Eq. (2).

$$|00\rangle \rightarrow |00\rangle; |01\rangle \rightarrow |01\rangle; |10\rangle \rightarrow |11\rangle; |11\rangle \rightarrow |10\rangle \quad (2)$$

Due to the capability of representing any multi-qubits gate by using a combination of CNOT gates and single-qubit gates, CNOT gates are frequently employed in quantum circuits for qubit state manipulation. A circuit consisting only of CNOT gates is called a CNOT circuit.

B. Quantum topology architecture

Although the number of qubits in NISQ devices has increased, they still face various physical constraints, including connectivity constraints and gate errors. The connectivity

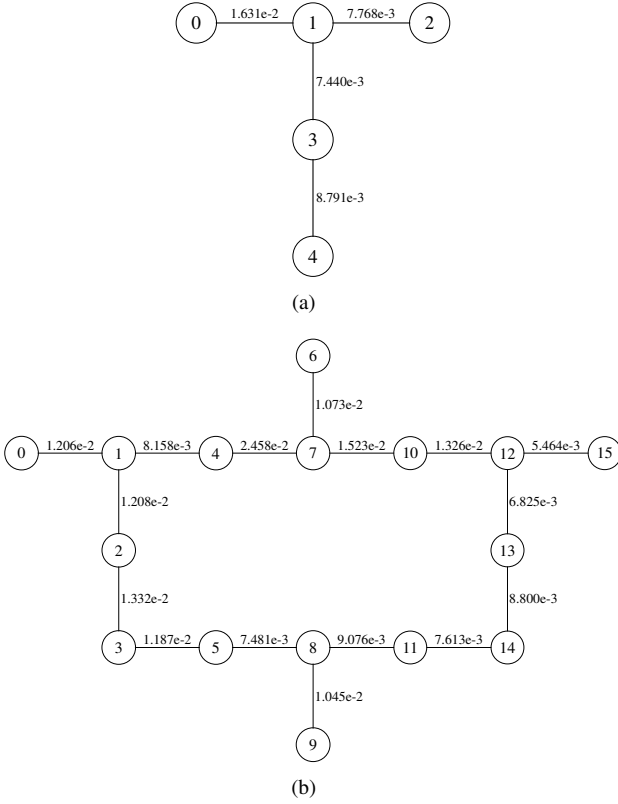


Fig. 2. Two coupling graphs of the IBMQ topology architecture. (a) The IBMQ_Quito topology with 5 qubits. (b) The IBMQ_Guadalupe topology with 16 qubits.

between different physical qubits can be represented by a quantum topology graph. Figure 2 displays the coupling graph of IBM's NISQ device topology, where each node represents a physical qubit and each edge represents the existence of an interaction path between qubits. Currently, the only two-qubit gate supported by IBM devices are CNOT gates, which can only operate on two qubits connected by an edge in the coupling graph. In other words, the logical qubits of the CNOT gate mapped onto these two connected physical qubits satisfy the NN constraint.

Another physical constraint reflected in the coupling graph is the gate error. The weights on the edges of the topological graph indicate the error rates of gate operations between two qubits. Higher weights imply higher error rates. Additionally, due to the qubit quality parameter, the error rate between two adjacent qubits is also different, which leads to different error rates for CNOT gates acting on different qubits. Therefore, it is necessary to satisfy the connectivity constraint and to reduce the gate error when mapping quantum circuits.

C. Boolean matrix

A CNOT gate can be represented by a unitary matrix of size 4×4 . The matrix of a CNOT circuit containing n qubits requires a tensor product of the individual CNOT's unitary matrix, so a CNOT circuit with n qubits requires a matrix representation of size $2^n \times 2^n$. However, in the Boolean matrix representation of a CNOT circuit, the matrix size corresponds

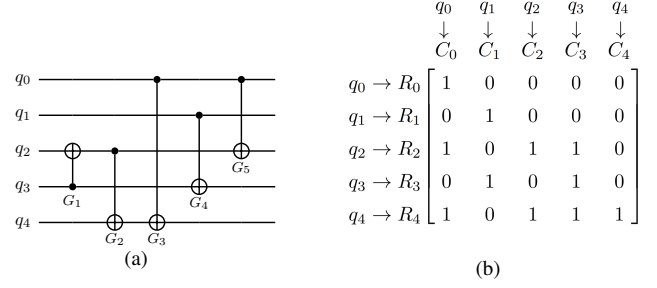


Fig. 3. A CNOT circuit and its Boolean matrix. (a) A CNOT circuit consisting of 7 CNOT gates. (b) Correspondence between the rows and columns of the Boolean matrix and the qubits.

to the number of qubits. A CNOT circuit with n number of qubits corresponds to an $n \times n$ Boolean matrix.

To calculate the Boolean matrix of a CNOT circuit, the following steps can be followed. For any CNOT gate with n variables in the circuit, where the variable domain is $\{x_1, x_2, \dots, x_i, \dots, x_j, \dots, x_n\}$, with x_i as the control bit and x_j as the target bit. In an $n \times n$ identity matrix, the row i corresponding to control bit x_i of each CNOT gate is XORed to the row j corresponding to the target bit x_j . This process is shown in Eq. (3).

$$\begin{array}{c}
 \begin{array}{c} C_0 \dots C_i \dots C_j \dots C_{n-1} \\ R_0 \\ \vdots \\ R_i \\ \vdots \\ R_j \\ \vdots \\ R_{n-1} \end{array}
 \begin{array}{c} \left[\begin{array}{cccc} 1 & \dots & \dots & 0 \\ \vdots & \ddots & \vdots & \vdots \\ 0 & \dots & 1 & \dots \\ \vdots & \vdots & \vdots & \ddots \\ 0 & \dots & \dots & 1 \\ \vdots & \vdots & \vdots & \vdots \\ 0 & \dots & \dots & \dots \\ \vdots & \vdots & \vdots & \vdots \\ 0 & \dots & \dots & 1 \end{array} \right] \\
 \xrightarrow{CNOT(i,j)} \\
 R_j \leftarrow R_j \oplus R_i
 \end{array}
 \begin{array}{c} \begin{array}{c} C_0 \dots C_i \dots C_j \dots C_{n-1} \\ R_0 \\ \vdots \\ R_i \\ \vdots \\ R_j \\ \vdots \\ R_{n-1} \end{array} \\ \left[\begin{array}{cccc} 1 & \dots & \dots & 0 \\ \vdots & \ddots & \vdots & \vdots \\ 0 & \dots & 1 & \dots \\ \vdots & \vdots & \vdots & \ddots \\ 0 & \dots & \dots & 1 \\ \vdots & \vdots & \vdots & \vdots \\ 0 & \dots & \dots & \dots \\ \vdots & \vdots & \vdots & \vdots \\ 0 & \dots & \dots & 1 \end{array} \right] \end{array}
 \end{array}
 \quad (3)$$

The CNOT circuit shown in Fig. 3(a) consists of seven CNOT gates with five qubits, namely $\{q_0, q_1, q_2, q_3, q_4\}$. It can be represented as a 5×5 Boolean matrix, where $\{q_0, q_1, q_2, q_3, q_4\}$ correspond to $\{R_1, R_2, R_3, R_4, R_5\}$ and $\{C_1, C_2, C_3, C_4, C_5\}$ in the Boolean matrix, respectively. During the conversion process of Boolean matrix, several XOR operations are performed. Firstly, the control bit q_3 of G_1 gate is XORed to the target bit q_2 and the result is stored in the target bit q_2 , which is expressed as $R_2 = R_2 \oplus R_3$ in the Boolean matrix. And then the control bit q_2 of G_2 gate is XORed to the target bit q_3 , which is expressed as $R_3 = R_3 \oplus R_2$ in the Boolean matrix. The same operation is carried out for G_3 to G_7 . The final Boolean matrix is shown in Fig. 3(b).

III. KEY-QUBIT PRIORITY INITIAL MAPPING STRATEGY

In order to extend the synthesis method with Hamiltonian path architectures, and solve the NN synthesis problem of CNOT circuits on the architecture without Hamiltonian paths, an approach is proposed to achieve the NN synthesis of CNOT quantum circuits while ensuring the NN constraint. This section proposes a key-qubit priority mapping model that prioritizes and maps key qubits on a coupling graph. Additionally, tabu search is employed to optimize the initial

mapping, aiming to reduce the number of CNOT gates and enhance the circuit fidelity.

A. Key-qubit priority model

The synthesis of CNOT circuits can be accomplished by using Gaussian elimination and the Steiner tree model to convert the Boolean matrix M of the CNOT circuit to an identity matrix I . Each row or column operation in the Gaussian elimination that converts M to I corresponds to a CNOT gate. The inverse cascade of these CNOT gates is equivalent to the original circuit. The Boolean matrix is an $n \times n$ matrix divided into n layers diagonally. The first layer includes the first column and the first row, the i^{th} layer ($1 \leq i \leq n$) includes the i^{th} column and the i^{th} row until the last layer contains the unique element 1.

Definition 1. During the procedure of Gaussian elimination, a CNOT gate is utilized to convert an element S_i from 0 to 1 by using an element S_j of a column of the matrix. This operation is referred to as setting 1 and represented as $set1[S_i, S_j]$, as it performs the operation $0 \oplus 1 = 1$. Likewise, the operation of setting 0, which involves applying a CNOT gate to obtain $1 \oplus 1 = 0$, is denoted as $set0[S_i, S_j]$.

Based on the preceding elimination rules, the Boolean matrix M must be processed sequentially by column. A Steiner tree is constructed for each i^{th} column of the matrix. The $set1$ or $set0$ operation is then employed to convert all non-zero elements in each column to 0, except for the i^{th} element, which is transformed to 1.

Example 1. Taking the circuit in Fig. 3(a) as an example, the circuit is mapped onto the coupling graph in Fig. 2(a) in the default initial mapping $\{q_0 \rightarrow Q_0, q_1 \rightarrow Q_1, q_2 \rightarrow Q_2, q_3 \rightarrow Q_3, q_4 \rightarrow Q_4\}$. The first column of the Boolean matrix M , which represents this circuit, is processed first. A Steiner tree is constructed for the elements of the first column. In this Steiner tree, q_0 acts as the root node, and q_2 and q_4 are the leaf nodes. The Steiner tree is then post order traversed, and the sequence of qubits elimination is q_4, q_2, q_0 . While eliminating q_4 , it is not possible to convert q_4 to 0 by using $set0(q_4, q_3)$ because the state of q_3 , which is adjacent to q_4 , is 0. Therefore, $set1(q_3, q_4)$ is used to convert q_3 to 1, followed by the execution of $set0(q_4, q_3)$. The corresponding CNOT operations are CNOT(4,3) and CNOT(3,4). Similarly, the same operation is performed on the other qubits until only q_0 is 1 in the first column of this matrix. The process of synthesis of the first column is shown in Fig. 4. The numbers indicate the order of the set operations, the solid arrows indicate $set1$, the dashed arrows indicate $set0$.

The elimination rule in Boolean matrix transformation requires that the matrix be processed in column order. As per this rule, the operation paths in the corresponding coupling graph are: $[q_0 \rightarrow q_1 \rightarrow \dots \rightarrow q_i \dots \rightarrow q_n]$. The corresponding coupling graph needs to remove the vertex q_i in every i^{th} step. This method is only applicable to architectures with Hamiltonian paths. However, in architectures without Hamiltonian paths, the vertex removal step may cause the coupling graph to be

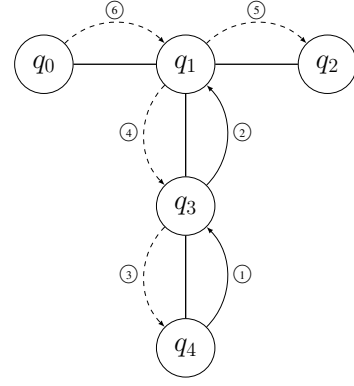


Fig. 4. The NN synthesis process in the IBMQ_Quito architecture. The numbering indicates the order of the sets, the dotted arrows indicate $set0$, the solid arrows indicate $set1$.

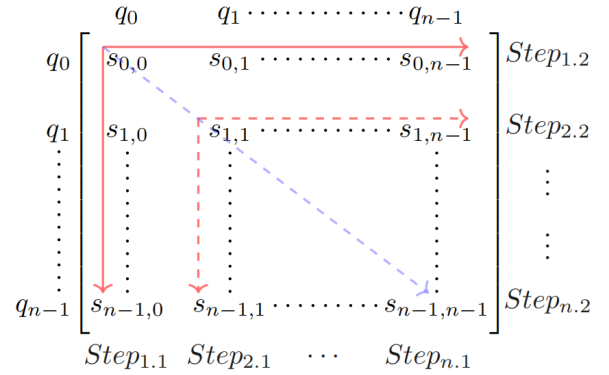


Fig. 5. Illustration of the Boolean matrix elimination process. The Boolean matrix is processed by layer and follows the principle of columns before rows.

split into two disconnected subgraphs. As a result, some of the qubits may lose their interaction paths with each other, making it impossible to use this part of the vertices for $set0$ or $set1$ operations in the subsequent synthesis process. Ultimately, this method results in the circuit that cannot be synthesized.

To solve this problem, the principle of layer precedence is followed in the Boolean matrix elimination process. The layer-by-layer elimination approach avoids the dependence of subsequent elimination steps on the deleted vertices. Thus, the matrix elimination starts from the first layer and ending at the $n - 1$ layer, as shown in Fig. 5. In each layer, the Boolean matrix is first eliminated by column and then by row. A Steiner tree is constructed based on each row or column, and all the 1s except the diagonal elements are converted to 0s by Gaussian elimination and Steiner methods. This ensures that the diagonal elements of the matrix after each previous layer operation will not be affected by the subsequent synthesis process. Topological constraints need to be satisfied in the conversion process. The final reduction yields an identity matrix, and the quantum circuit corresponding to the Boolean matrix is the inverse cascade of the CNOT gates applied during all transformations.

Lemma 1. Let $G = (V, E)$ be an undirected graph. If the removal of a vertex $v \in V$, along with all the edges associated with it, causes G to split into two or more disconnected

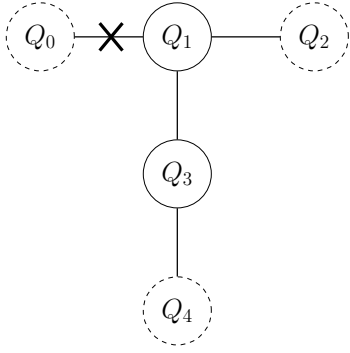


Fig. 6. An example of key-qubit priority model for the IBMQ_Quito. The dashed qubits are non-cutting points, i.e., key qubits. Solid qubits are cut points.

subgraphs, then the vertex v is known as the cut point of graph G [26].

In the coupling graph shown in Fig. 6, Q_1 and Q_3 are cut points. Their deletion from the coupling graph results in the splitting of the graph into multiple subgraphs, rendering the matrix elimination process infeasible. In order to perform matrix elimination operations accurately, it is necessary to map logical qubits with lower indexes to vertices that are not cut points in the physical quantum coupling graph in priority during the initial mapping. We refer to such vertices as key qubits.

Definition 2. For a coupling graph $G = (Q, E)$ that contains several physical qubits, where $Q = \{Q_0, Q_1, \dots, Q_i, \dots, Q_{n-1}\}$ ($0 \leq i < n$), a vertex Q_i that is a non-cut point is regarded as the key physical qubit of the priority mapping, or the key qubit for brevity.

To ensure the feasibility of matrix elimination, priority is given to the physical qubits that are non-cut points, known as key qubits, during the mapping process. For instance, in the IBMQ_Quito architecture, qubits Q_0 , Q_2 , and Q_4 are non-cutting points, which are the key qubits, as shown in Fig. 6. During the initial mapping, priority is given to map q_0 , q_1 , q_2 to these three physical qubits. If q_0 is the first qubit to be mapped to Q_0 , it becomes disconnected from the other qubits in the coupling graph after the first layer of matrix elimination is completed. By prioritizing the constraints of mapping key qubits, the key-qubit priority model can be satisfied while reducing the complexity of the initial mapping at the same time.

B. Key-qubit priority mapping based on tabu search

In order to avoid the occurrence of disconnected subgraphs in coupling graph, this paper proposes a key-qubit priority mapping method. This method prioritizes the vertices that are not cut points, i.e., key points, on the coupling graph. Then the processed vertices and the edges connected to them are removed from the coupling graph until a complete Hamiltonian path exists in the updated coupling graph. After the deletion of a key qubit, a new subgraph is created. New key qubits may appear in this subgraph, which were not cut points in the

original coupling graph. By considering the constraints of key qubits, a recursive algorithm for selecting and mapping the key qubits in the order of increasing logical qubits index can be provided in the analysis of the key-qubit priority model. This ensures that the logical qubits at the key qubits are prioritized in the subsequent elimination process. The key-qubit priority initial mapping algorithm KQPIM is shown in Algorithm 1.

Algorithm 1: Key-qubit priority initial mapping (KQPIM)

Input: The coupling graph $G = (V, E)$, the initial map π , the number of logical qubits n , the list of initial key qubits $ikey_list$

Output: The initial map π_0

```

1 begin
2    $i \leftarrow \text{Nodes}(G_0) - \text{Nodes}(G)$ ;
3   if  $G \ni \text{Hamilton path}$  then
4     foreach  $Q_i$  in  $\text{Hamilton path}$  do
5       add  $\{i : Q_i\}$  to  $\pi$ ;
6        $i++$ ;
7     end
8     return  $\pi$ ;
9   end
10  if  $\pi = \text{null}$  then
11     $key\_list \leftarrow ikey\_list[0]$ ;
12     $G \leftarrow G/ikey\_list[0]$ ; /* Delete point
13    from  $G$  */
14  end
15  foreach  $Q$  in  $V$  do
16     $key\_list \leftarrow Q$  is non-cut points;
17  end
18  if  $G \nexists \text{Hamilton path}$  then
19     $key\_qubit \leftarrow key\_list[\text{random}]$ ;
20    add  $\{i : key\_qubit\}$  to  $\pi$ ;
21     $G \leftarrow G/key\_qubit$ ;
22     $i++$ ;
23  end
24  if  $\text{len}(\pi) \neq n$  then
25    KQPIM( $G, \pi, n, ikey\_list$ );
26 end

```

This algorithm takes the coupling graph G and the number of logical qubits n as input, and outputs a randomized key-qubit priority initial mapping. This algorithm takes the non-cut points in the coupling graph as key qubits and iterates through recursion, reducing the complexity of the initial mapping. However, it is worth noting that Algorithm 1 only outputs a single mapping scheme. With n qubits in a quantum computing architecture, there can be up to $n!$ possible initial mapping schemes, making it impractical to traverse each one by the brute force search method. Although the key-qubit priority initial mapping algorithm can reduce the search space of initial mappings, it may still not be able to find the optimal initial mapping quickly considering the increasing size of physical qubits on quantum computing devices. In this case, a better balance between solution accuracy and speed can be achieved

with the help of metaheuristic algorithms.

This work utilizes a tabu search algorithm to solve the initial mapping problem for CNOT circuit synthesis. Tabu search guides the search toward a more optimal region of the search space by maintaining a tabu table, while avoiding exploring suboptimal solutions previously. The algorithm iterates and updates the tabu table as it explores the solution space, gradually improving the quality of the found solution until a satisfactory solution is found or the maximum number of iterations is reached. Since the elimination of the Boolean matrix under topological constraints requires considering not only the CNOT cost under the NN constraint but also the overall fidelity of the circuit. The number of CNOT gates is highly correlated with the connectivity of the qubits in the coupling graph. Low qubits connectivity can necessitate more CNOT gates to complete the NN. On the other hand, the error rate of CNOT gates is a crucial factor affecting the fidelity of the circuit. Choosing qubits with a lower error rate for mapping is beneficial for building circuits with high fidelity.

The inter-vertex connectivity factor is one of the indicators of the connectivity between vertices in a graph. It ranges from 0 to 1, where 0 indicates that two vertices are not connected. A higher connectivity coefficient indicates stronger connectivity and fewer CNOT gates required to act on the two qubits. The connectivity factor can be calculated by using the Betweenness Centrality algorithm in graph theory [27]. The objective function F_π of the optimization method is defined in Eq. (4),

$$F_\pi = \prod_{0 \leq i < j < n} \frac{\sum_{v \neq i, j} \frac{C_v(i, j)}{C_v}}{C_{ij}} + \sum_{m=0}^{n-1} (m+1) \frac{\sum_{w \in E(\pi_m)} w}{|E(\pi_m)|} \quad (4)$$

where n denotes the number of qubits, $C_v(i, j)$ denotes the number of shortest paths through vertex v that contain both vertices i and j , C_v denotes the number of shortest paths through vertex v , C_{ij} denotes the number of shortest paths through i and j . m denotes the index number in the mapping method π , π_m denotes the m^{th} physical qubit in the mapping method π , $E(\pi_m)$ denotes the edge connected to the qubit π_m in the coupling graph, and w denotes the weight on this edge, i.e., the error rate.

The first half of Eq. 4 represents the degree of connectivity of the mapped qubits. This part is used to measure the connectivity of the sub-coupling graph when the physical qubits are not fully mapped. And the second half of Eq. 4 represents the fidelity profile of the mapped qubits. According to the key-qubit priority model, the more advanced qubits in π are removed first, the error rate associated with these qubits also have less impact on the circuit. To distinguish the importance of the error rates between different qubits, $m+1$ is assigned as the weight of these error rates. The later the qubits in π are removed, the greater the number of CNOT gates acting on these qubits, and so the greater the weight set on these qubits.

After the cost function has been determined, the initial mapping of CNOT circuit synthesis is optimized by tabu search algorithm. Firstly, a tabu table of length N is initialized, and the mapping method π_0 of Algorithm 1 (KQPIM) is added to the

tabu table. Secondly, a set of candidate solutions is generated, namely multiple mapping methods $\pi_\Delta = \{\pi_1, \pi_2, \dots, \pi_n\}$, by randomly disturbing the initial key qubits in π_0 . These initial key qubits are the non-cut points of the uncut coupling graph, and these qubits form the `ikey_list`. Disturbing only the `ikey_list` ensures that the key qubit priority model is satisfied. Next, the mapping schemes in π_Δ that already exist in the tabu table are removed, and the mapping schemes whose cost F_π is lower than the average cost in the tabu table are added to the tabu table. Finally, the tabu table is updated to remove the mappings with higher cost F_π in the tabu table. This cycle continues until the end of the iteration. The pseudo-code for the tabu search algorithm to optimize the initial mapping of CNOT circuit synthesis is provided in Algorithm 2.

Algorithm 2: Key-qubit priority initial mapping optimization (KQPIMO)

Input: The coupling graph $G = (V, E)$, the number of logical qubits n

Output: The best initial map π_{best}

```

1 begin
2    $T\_list \leftarrow [] * N, \pi \leftarrow []$ ;
3    $ikey\_list \leftarrow$  non-cut points in  $G$ ;
4    $\pi_0 \leftarrow KQPIM(G, \pi, n, ikey\_list)$ ;
5   add  $\pi_0$  to  $T\_list$ ;
6   for  $i < iterations$  do
7      $\pi_\Delta \leftarrow []$ ;
8     for  $k = 0$  to  $N$  do
9       // Change only key qubits
10       $ikey\_list \leftarrow$  random disturbance key qubits
11      in  $ikey\_list$ ;
12       $\pi_k \leftarrow KQPIM(G, \pi, n, ikey\_list)$ ;
13      add  $\pi_k$  to  $\pi_\Delta$ ;
14    end
15    foreach  $\pi$  in  $\pi_\Delta$  do
16      if  $\pi \notin T\_list$  and  $F_\pi \leq F_{avg}(T\_list)$  then
17        | add  $\pi$  to  $T\_list$ ;
18      end
19      if  $size(T\_list) > N$  then
20        |  $T\_list \leftarrow update(T\_list)$ 
21      end
22    end
23  end
24   $\pi_{best} \leftarrow best(T\_list)$ ;
25  return  $\pi_{best}$ ;

```

The key-qubit priority initial mapping optimization algorithm based on tabu search described above is an iterative optimization method. It helps to improve the optimization rate and fidelity of quantum circuits by setting a reasonable length of the tabu table and the number of iterations. This enables the mapping method to trade off a certain amount of time cost for the enhancement of the overall quality of the circuit.

IV. KEY QUBIT-AWARE CNOT CIRCUIT NN SYNTHESIS

This section presents an NN synthesis method based on the key-qubit priority initial mapping strategy. The method improves the synthesis efficiency by prioritizing the mapping and elimination processing of key qubits. It enables the implementation of CNOT circuit NN synthesis on an architecture with and without Hamiltonian paths. And at the same time, the fidelity of the NN synthesized circuits is improved as much as possible. Specifically, the target-aided row matching algorithm is introduced firstly, which helps to find the best auxiliary row to achieve row elimination of Boolean matrix. Next, this section describes the noise-aware CNOT circuit NN synthesis algorithm based on layer convergence, which uses a layer-by-layer elimination method. Finally, an algorithm example is provided to facilitate a better understanding of the application and effect of the algorithm.

A. Target-assisted row matching algorithm

In the key-qubit priority mapping model, the processed vertices need to be removed from the coupling graph. Consequently, the elimination must process not only the current column but also the current row. In order to change the values of the elements in the current row other than those on the main diagonal to 0, it is necessary to use the auxiliary of other rows in the matrix to perform an XOR operation with the current row. The set of target aided rows found based on the current row is presented in Definition 3.

Definition 3. In an invertible Boolean matrix, suppose the current row is R_i , and its corresponding unit row vector is denoted as e_i , where $\forall e_{ij} \in e_i$, $e_{ij} = 1$ if $j = i$, and $e_{ij} = 0$ otherwise. The set Set_k that satisfies $\sum R_k = R_i + e_i (i < k \leq n, n = r(R))$ in the matrix is referred to the target-aided rows set.

Example 2. Figure 7 illustrates an example of matching the target-aided rows. At this point, the rows of the first layer and the columns of the second layer of this matrix have been processed, and the next step is to complete the row elimination of the second layer. According to Definition 3, it is necessary to match to the set of target-aided rows that satisfy the condition $\sum R_j = R_1 + e_1$, where $e_1 = [0, 1, 0, 0, 0]$. By calculating $R_1 + e_1 = [0, 0, 1, 0, 1]$, the set of target-aided rows must be matched to obtain $\sum R_j = [0, 0, 1, 0, 1]$. And the set $\{R_3, R_4\}$ satisfies $R_3 + R_4 = [0, 0, 1, 0, 1]$, therefore, the target-aided rows set of R_1 is $\{R_3, R_4\}$.

In the case where the matrix is invertible, the system of linear equations $Ax = y$ must have a unique solution. Therefore, if the target row exists, the set of target-aided rows must be found, i.e., the target-aided row matching is completed. Specifically, the set of target rows can be determined by solving the system of linear equations. If the system of linear equations has a solution, it means that the target row set exists, and we only need to find the rows corresponding to the non-zero elements in the solution vector. Based on the above analysis, a target-assisted row matching algorithm is given, as shown in Algorithm 3.

$$\begin{array}{c}
 q_0 \\
 q_1 \\
 q_2 \\
 q_3 \\
 q_4
 \end{array}
 \begin{bmatrix}
 1 & 0 & 0 & 0 & 0 \\
 \mathbf{0} & \mathbf{1} & \mathbf{1} & \mathbf{0} & \mathbf{1} \\
 0 & 0 & 0 & 1 & 0 \\
 0 & 0 & 1 & 0 & 0 \\
 0 & 0 & 0 & 0 & 1
 \end{bmatrix}
 R_1 + e_1 = R_3 + R_4$$

Fig. 7. Target Auxiliary Row Matching Example.

Algorithm 3: Goal-aided row matching (GARM)

Input: The invertible boolean matrix M , the target row index i

Output: The target auxiliary row index list R_j

```

1 begin
  // Get the rank of the matrix
2   $n \leftarrow r(M)$ ;
  // Initialize list to generate
  permutations
3   $L \leftarrow [], R\_list \leftarrow []$ ;
4  for  $m = i$  to  $n$  do
  // Generate the index sequence
  to be matched according to
  the target row index
5  add  $m$  to  $L$ ;
6  end
7  for  $length = i$  to  $n$  do
  // save current permutation
8   $R\_list \leftarrow \text{Perm.append}(L, length)$ ;
9  end
10 foreach  $R_j$  in  $R\_list$  do
11  if  $\sum R_j = R_i + e_i$  then
12  | return  $R_j$ ;
13  end
14 end
15 end

```

To construct the set of target-aided rows, the algorithm first generates the sequence of indexes to be matched in accordance with the target row index. Next, the algorithm searches for feasible solutions through the full permutations of all rows, except for the target row. The full permutation from m to n can be expressed as $\text{Perm}(L, n)$, where L denotes any integer set that is not empty and n denotes the full permutation of n numbers from L . The complexity of Perm is shown in Eq. (5).

$$O\left(\sum_{i=0}^n \frac{n!}{(n-i)!}\right) = O\left(n! \sum_{i=0}^n \frac{1}{i!}\right) \quad (5)$$

where n denotes the number of qubits. The value of $\sum_{i=0}^n \frac{1}{i!}$ in Eq. (5) must be less than 3, and it is a constant. Therefore, the overall complexity of the algorithm is $O(n \cdot n!)$.

B. Noise-aware CNOT circuits NN synthesis strategy

The NN synthesis algorithm for CNOT circuit can be obtained based on the key-qubit priority initial mapping optimization algorithm and the target-aided row matching algorithm by using the Boolean matrix transformation method under topological constraints. Given that quantum algorithms involve many two qubit operations, the error of each two-qubit operation, i.e., two-qubit gate, is more significant compared to single-qubit operations. In order to maximize the probability of successful execution of the synthesized CNOT circuits on real quantum computing devices, the error of each inserted CNOT gate must be considered during the synthesis of CNOT circuits. A noise-aware CNOT circuit mapping method is proposed to mitigate these unavoidable noise problems.

In the process of matrix elimination, multiple interaction paths may occur when Gaussian elimination is performed between two qubits that are not close neighbors. Since the error rates between neighboring qubits on different paths are different, choosing different interaction paths to build Steiner tree can cause different errors in the results. To measure the error cost of each interaction path, we propose an interaction path fidelity measure F_{path} , as shown in Eq. (6).

$$F_{path} = \prod_{Q_i, Q_j \in path} (1 - E[Q_i][Q_j]) \quad (6)$$

where Q_i and Q_j are the two qubits that are near neighbors on the interaction path, and $E[Q_i][Q_j]$ denotes the two-qubit gate operation error rate, i.e., the weight of the edge on the coupling graph. A larger F_{path} indicates a higher fidelity on this interaction path, which means that the integrated CNOT quantum circuit can obtain a better reliability.

The interaction path selection problem can be transformed into a search for the path with the highest metric F_{path} among all paths between two qubits. This problem can be solved by Dijkstras algorithm. The two qubits of the *set0* or *set1* action are used as the start and finish qubits in the interaction path selection strategy based on the Dijkstras algorithm. The strategy visits adjacent qubits from the start qubit and calculates F_{path} , then looks for higher F_{path} vertices until the end qubit is visited. When there is only one interaction path between the start qubit and the end qubit, this path is the one with the highest F_{path} . This path selection strategy provides an interaction path with the highest fidelity for two logical qubits that are not adjacent to each other, so that the set operation acting on this interaction path has the lowest error rate and reduces the effect of errors in the matrix elimination process.

Example 3. Suppose a circuit is mapped to the coupling graph in Fig. 2(b), and the two qubits mapped to Q_7 and Q_9 need to be eliminated, where the qubit mapped to Q_7 is the main diagonal element and the qubit mapped to Q_9 is 1 in the matrix. So Q_7 is the root node of the Steiner tree, and Q_9 is the child node. Since Q_7 and Q_9 are not adjacent, the *set0* operation cannot be directly performed. Therefore, it is necessary to gradually apply *set1* to all qubits on the path from Q_7 to Q_9 . At this point, there are two interactive paths available, $path_1$ is (7-4-1-2-3-5-8-9), and $path_2$ is (7-10-12-13-14-11-8-9). The two interaction paths are shown in

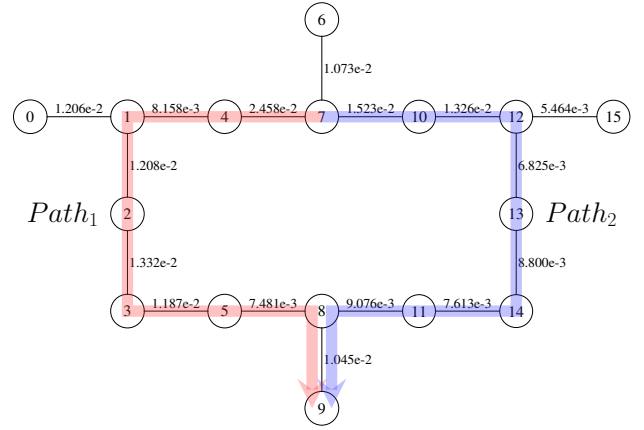


Fig. 8. Two interaction paths between Q_7 and Q_9 in the IBMQ_Guadalupe.

Fig. 8. To determine the optimal path, we calculate F_{path_1} and F_{path_2} respectively, and find that F_{path_2} is greater than F_{path_1} . Therefore, $path_2$ is selected as the interactive path.

A minimum spanning tree for elimination is built by using the Steiner tree method, with the primary diagonal element serving as the root node. Vertices with a value of 1 in the current row or column are processed in turn, and the least weighted interaction path between these vertices and the tree is identified. All vertices on the path are then added to the tree until it contains all vertices with a value of 1. The minimum spanning tree obtained based on the above-mentioned method is referred to as a minimum noise Steiner tree (MNST). Once minimum noise Steiner trees have been constructed for each row or column of the matrix, the matrix can be eliminated. The key-qubit priority initial mapping algorithm ensures the connectivity between the qubits during the matrix transformation. The target row matching algorithm solves the problem of finding the set of auxiliary rows of the elimination elements when processing row elimination elements. The specific flow of the NN synthesis algorithm for CNOT circuits on the general architecture is shown in Algorithm 4.

The algorithm processes the row and column of the current main diagonal element according to the layer convergence direction. First, the algorithm generates the initial mapping method π by algorithm 3 (line 3). When processing column elements, the algorithm generates a minimum noise Steiner tree based on the elements with a value of 1 in the current column (line 6). If a Steiner point exists, the child node is used to set the Steiner point to 1 (lines 8-14), and then the algorithm performs a post-order traversal to remove the main diagonal elements by *Set0* (lines 15-19). When processing row elements, the algorithm employs the target auxiliary row matching algorithm to find the row set used to assist elimination (line 20). Then a Steiner tree is generated based on the current row and the auxiliary row set (line 21). If a Steiner point exists, the algorithm uses the child node to set the Steiner point to 1 by *Set1* (lines 23-29). And finally, the algorithm sets the elements of the current row except the main diagonal to 0 by traversing the Steiner tree in post order (lines 31-35). After processing the row and column corresponding to the current

Algorithm 4: Nearest Neighbor Synthesis Algorithm for CNOT Quantum Circuits Based on Layer Convergence (LCNNS)

Input: The boolean matrix M , the qubit coupling diagram $G = (V, E) (|V| = n)$

Output: The CNOT gate sequence applied in row operation

```

1 begin
2    $CNOT\_list \leftarrow []$ ;
3    $\pi \leftarrow KQPIMO(G, n)$ ;
4    $V\_list \leftarrow \pi$ ;
5   foreach  $i$  in  $V\_list$  do
6     // Minimum noise Steiner tree
       implemented by Dijkstra
7      $T \leftarrow MNST(G, j | M_{ji} = 1)$ ;
8      $col\_post\_list \leftarrow$  postorder traverse  $T$  from  $i$ ;
9     // Set the points in  $T$  with a
       value of 0 to 1
10    foreach  $c$  in  $col\_post\_list$  do
11       $k \leftarrow c.parent$ ;
12      if  $M_{ki} = 0$  and  $M_{ci} = 1$  then
13         $M_k \leftarrow M_k \oplus M_c$ ;
14         $CNOT\_list.append([c, k])$ ;
15      end
16    end
17    // Set points in  $T$  other than
       the root node to 0
18    foreach  $c$  in  $col\_post\_list$  do
19       $l \leftarrow c.children$ ;
20       $M_l \leftarrow M_l \oplus M_c$ ;
21       $CNOT\_list.append([c, l])$ ;
22    end
23     $S_j \leftarrow GARM(M, i)$ ;
24     $T' \leftarrow S_j \cup i$ ;
25     $row\_pre\_list \leftarrow$  preorder traverse  $T$  from  $i$ ;
26    // Set the points in  $T'$  with a
       value of 0 to 1
27    foreach  $r$  in  $row\_pre\_list$  do
28      if  $r \notin S_j$  then
29         $k \leftarrow r.parent$ ;
30         $M_k \leftarrow M_k \oplus M_r$ ;
31         $CNOT\_list.append([r, k])$ ;
32      end
33    end
34     $row\_post\_list \leftarrow$  postorder traverse  $T$  from  $i$ ;
35    // Set points in  $T'$  other than
       the root node to 0
36    foreach  $r$  in  $row\_post\_list$  do
37       $k \leftarrow r.parent$ ;
38       $M_k \leftarrow M_k \oplus M_r$ ;
39       $CNOT\_list.append([r, k])$ ;
40    end
41    // remove qubit  $i$  from  $G$ 
42     $G \leftarrow G/i$ ;
43  end
44  return  $CNOT\_list$ ;
45 end

```

qubit, the algorithm removes the current qubit and the edges connected to it from the coupling graph (line 36). Throughout the elimination process, the CNOT gate corresponding to each row and column operation is recorded.

The following is the complexity analysis, let n be the number of qubits in the coupling graph. The Steiner tree is generated by the Dijkstra algorithm (line 5), and the time complexity is $O(n^2)$. The time complexity of traversing the Steiner tree (line 6) is $O(n^2)$. The operations in the first foreach loop (lines 7-11) have constant time complexity, so the time complexity of the foreach loop is $Q(n)$. Similarly, the time complexity of the foreach loop (line 14) is also $Q(n)$. The time complexity of the GARM algorithm (line 19) is $Q(n \cdot n!)$. A new tree is constructed by using the Prim algorithm (line 20), and the time complexity is $O(n^2)$. The time complexity of obtaining the preorder traversal list (line 21) is $Q(n)$. The time complexity of the two foreach loops (lines 22 and 30) are both $Q(n)$. The time complexity of traversing the list (line 28) is $O(n^2)$. So the total time complexity of algorithm 4 is shown in Eq. (7).

$$O(n(n^2 + n^2 + n + n!n + n^2 + n + n^2 + n)) = O(4n^3 + n^2n! + 4n) \quad (7)$$

where n represents the number of qubits in the coupling graph. In summary, the time complexity of Algorithm 4 is dominated by the time complexity of the GARM algorithm. The complexity is further simplified to $O(n^2n!)$.

C. Algorithm example

To illustrate the NN synthesis process, we consider the CNOT circuit shown in Fig. 3(a) and use the IBMQ_Quito architecture as an example. The synthesis process is presented in Fig. 9. According to the key-qubit priority initial mapping optimization algorithm, the initial mapping $\{q_0 \rightarrow Q_0, q_1 \rightarrow Q_4, q_2 \rightarrow Q_3, q_3 \rightarrow Q_1, q_4 \rightarrow Q_2\}$ that satisfies the key-qubit priority model is obtained.

First, the algorithm process the first row of the first column. The first column of the 1 element corresponding to the qubits q_0, q_2, q_4 . The Steiner tree is generated in the coupling graph, and the algorithm performs post-order traversal of the current Steiner tree. If the current node value is 1 and the parent node value is 0, the current node is used to set its parent node to 1. So q_4 is used to set q_3 to 1 first, and CNOT(4,3) is executed. Next, the entire Steiner tree is traversed posteriorly, and q_4, q_2 , and q_3 are traversed in order to apply the parent node of the current node to the current row, i.e., CNOT(3,4), CNOT(3,2), and CNOT(0,3) are applied. Because the first row is already a unit vector, there is no need to process the first row.

Next, the second column and the second row are processed. The qubits corresponding to the 1 element in the second column are q_1, q_2, q_3, q_4 . The Steiner tree is generated in the coupling graph, and the current Steiner tree is traversed in the post-order. There are no Steiner points in the current Steiner tree, so no operation is needed. Then, the algorithm post-order traverses the whole Steiner tree, traverse q_4, q_3, q_2 in turn, and apply the row where the parent node of the current node is located to the current row, i.e., apply CNOT(3,4), CNOT(3,2),

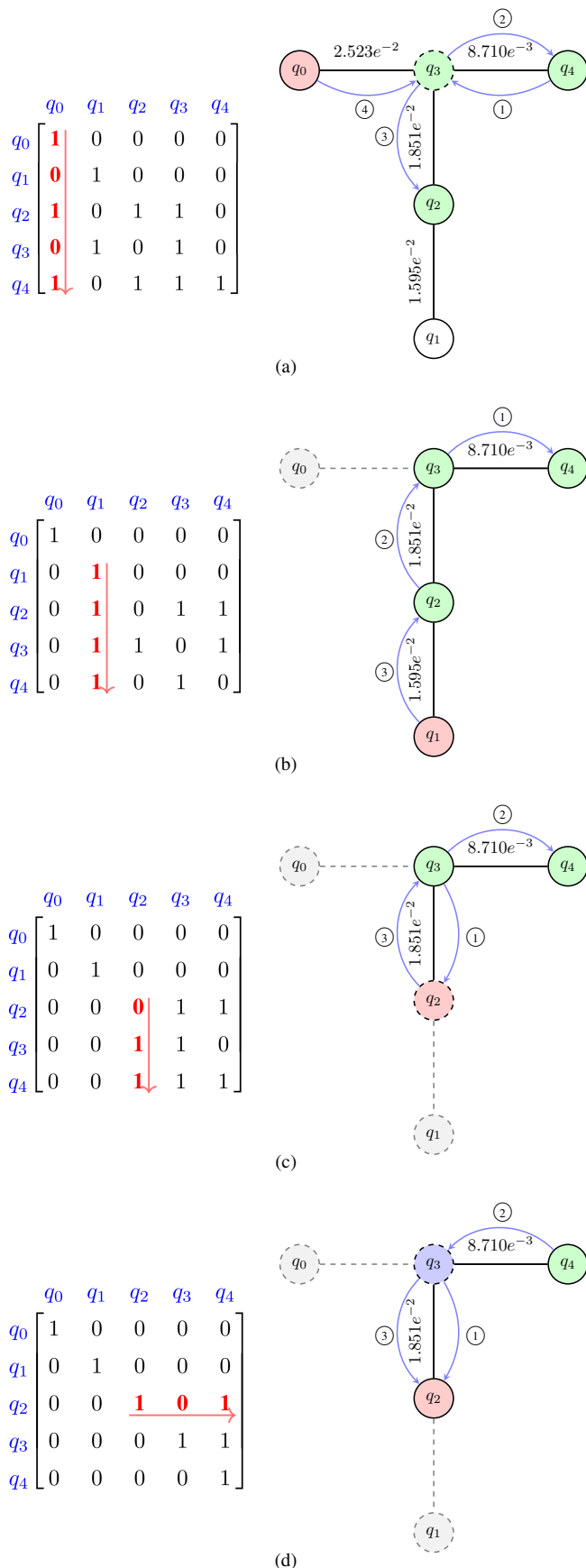


Fig. 9. Example of synthesis process for the circuit in Fig. 3(a).

CNOT(1,2). Since the second row is already a unit vector, there is no need to process the second row.

Finally, the third column and the third row are processed. The qubits corresponding to the 1 element in the third column are q_3 and q_4 . The Steiner tree is generated in the coupling graph, and the current Steiner tree is traversed in the post-order. The qubit q_3 is used to set q_2 to 1 first, and then apply CNOT(3,2). Then, the algorithm traverses the whole Steiner tree in post-order, traverse q_4 and q_3 in turn, and apply the row where the parent node of the current node is located to the current row, that is, apply CNOT(3,4), CNOT(3,2). At this point, the third row is not a unit vector and needs to be processed. By using the target-aided row matching algorithm, the third row can be obtained from the fifth row and the unit matrix $e_i=[0,0,1,0,0]$. So the Steiner tree is generated based on q_2, q_4 . After first preorder traversal of the Steiner tree, because q_3 is not in the set of target rows, it is necessary to apply the corresponding row of q_3 to the corresponding row of q_4 , i.e., apply CNOT(3,4). Then the algorithm post-order traverses the Steiner tree, traverse q_4 and q_3 in turn, and apply the row where the current node is located to the row where the parent node is located, i.e., apply CNOT(4,3), CNOT(3,2). At this point, the whole matrix becomes a unit matrix, and the NN synthesis ends.

V. EXPERIMENTAL RESULTS AND ANALYSIS

The algorithms in this section are all implemented in Python language, and the experimental environment is macOS Big Sur (11.2.3) operating system with Apple M1 Pro octa-core processing and 16GB RAM. The experiments in this section consist of three parts. First, the selected quantum circuits are the 5-qubit random CNOT circuits provided in [18], corresponding to the gate levels of 2, 4, 5, 8, 10, 15, and 20, with 20 quantum circuits for each quantum gate level. Secondly, to verify the effect on the existing benchmark, a selection of benchmark circuits with gate levels ranging from 11 to more than 10,000 have been chosen. Finally, the synthesis of Bernstein-Vazirani algorithm is utilized to illustrate the generality of the proposed method.

A. Experimental results

To evaluate the effectiveness of the proposed CNOT circuit NN synthesis method on real quantum computing devices, all 5-qubit circuits are executed on IBMQ_Quito computing device of IBMQ. The HA method in [25] and the method proposed in this paper are tested separately to count the fidelity of each quantum circuit execution. The results of the first set of experiments are shown in Fig. 10. Since the circuits are relatively small, the average optimization rate is about 8%.

The second set of experimental data is the classical benchmark circuit, which is a widely recognized as a standard for evaluating the performance of quantum algorithms and quantum computers. The experimental data for this benchmark circuit is presented in Table I and Table II. And the corresponding data comparison graph is shown in Figs. 14-15. It is worth noting that in this study, four different methods were compared for synthesizing the CNOT circuit, namely

TABLE I
THE 5-QUBIT BENCHMARK EXPERIMENTAL DATA

NO.	Benchmark	CNOT	Qiskit			Tket			HA			LCNNS			Imp
			CNOT	Depth	Fidelity	CNOT	Depth	Fidelity	CNOT	Depth	Fidelity	CNOT	Depth	Fidelity	
1	4mod5-v1_22	11	23	22	0.7581	17	26	0.8002	18	18	0.6997	8	8	0.8334	1.04
2	4mod5-v1_24	16	38	36	0.6403	31	47	0.7418	38	35	0.6023	16	16	0.7087	0.96
3	mod5mils_65	16	31	31	0.7153	31	51	0.7097	35	35	0.7069	6	6	0.8277	1.16
4	alu-v0_27	17	43	39	0.5655	38	41	0.6049	39	33	0.6498	3	2	0.8664	1.33
5	alu-v3_35	18	37	35	0.6257	37	56	0.6434	37	35	0.6693	4	4	0.8519	1.27
6	alu-v4_37	18	37	35	0.627	39	43	0.5884	43	37	0.4484	8	6	0.771	1.23
7	4gt13_92	30	63	59	0.417	52	85	0.5464	61	58	0.4484	14	13	0.7412	1.36
8	4mod5-v1_23	32	71	69	0.558	66	104	0.5338	87	81	0.3419	12	12	0.7694	1.38
9	decod24-v2_43	32	50	50	0.6662	40	66	0.6953	50	50	0.618	1	1	0.8729	1.26
10	4gt5_75	38	77	75	0.4473	78	126	0.4905	90	81	0.3221	17	15	0.7472	1.52
11	4gt13_91	49	113	106	0.3487	87	141	0.4564	98	95	0.3569	13	11	0.7597	1.66
12	alu-v4_36	51	110	109	0.362	93	152	0.4842	112	104	0.3234	6	6	0.8086	1.67
13	4gt13_90	53	109	108	0.3645	95	148	0.4258	105	100	0.3234	16	14	0.7742	1.82
14	hwb4_49	107	221	218	0.1955	207	314	0.2482	261	248	0.1358	10	10	0.8408	3.39
15	mod10_171	108	246	240	0.1276	210	341	0.2332	259	243	0.2374	1	1	0.8696	3.66

Qiskit, Tket, HA and LCNNS. Qiskit is a quantum computing framework developed by IBM that can be used to build and simulate quantum circuits. Tket is a quantum compiler developed by Cambridge Quantum Computing that converts advanced quantum algorithms into quantum circuits. HA is a method proposed in [25], while LCNNS is the method proposed in our work. To ensure the fidelity and reliability of the synthesized CNOT circuit, various metrics need to be considered. In this regard, three performance metrics: CNOT gate number, circuit depth, and execution fidelity, were selected as control parameters for the experiments. The final improvement is the ratio of the fidelity of LCNNS to the highest fidelity among the other methods. A result greater than 1 indicates the presence of an optimization effect. The larger the ratio, the more significant the improvement. By comparing the experimental results of these four methods using the three performance metrics mentioned above, it is possible to evaluate the effectiveness and efficiency of the proposed algorithm and to identify areas for further improvement.

In the NISQ era of quantum computing, noise plays a more significant role than in classical computing due to the special nature of qubits, making fidelity optimization more crucial. Fifteen 5-qubit benchmarks are selected for testing in Table I, and all circuits in Table I are executed on IBMQ_Quito computing device of IBMQ. The fidelity of the circuits in Table I is optimized up to 1.647 times on average, which corresponds to a 64.7% optimization rate. Twelve benchmarks of 15 or 16 qubits are selected for the experiment in Table II, and the number of CNOT gates reached more than 10,000 in the largest quantum circuits. In contrast to the way fidelity is verified in Table I, the circuit fidelity results for benchmark in Table II are performed with the IBMQ simulator. In some circuits in Table II, the fidelity is optimized up to 100 times or more.

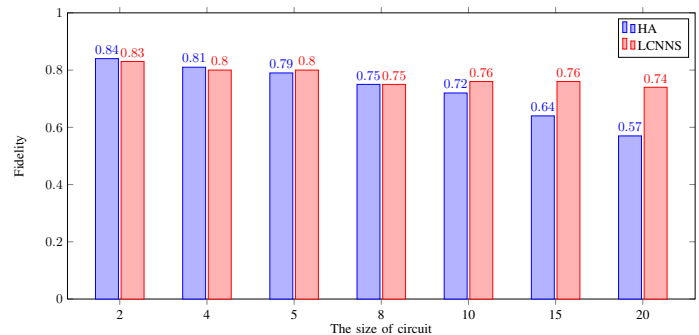


Fig. 10. 2-20 qubits scale circuit experimental data comparison with HA.

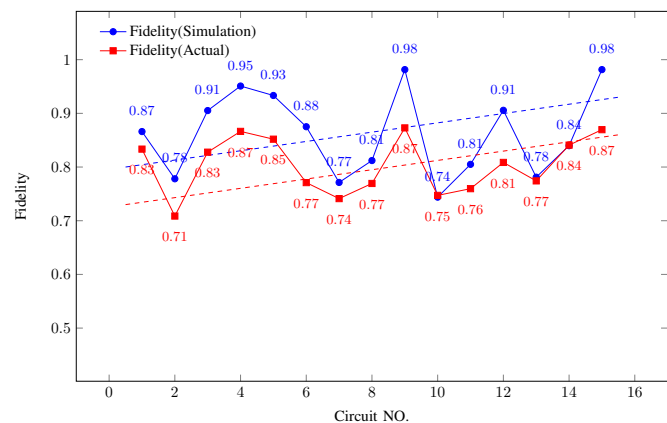


Fig. 11. Actual fidelity versus simulated fidelity in Table I.

TABLE II
THE 15-AND-16-QUBIT BENCHMARK EXPERIMENTAL DATA

NO.	Benchmark	CNOT	Qiskit			Tket			HA			LCNNS			Imp
			CNOT	Depth	Fidelity	CNOT	Depth	Fidelity	CNOT	Depth	Fidelity	CNOT	Depth	Fidelity	
16	cnt3-5_179	85	161	163	0.4362	63	53	0.442	308	212	0.281	36	31	0.7731	1.75
17	rd84_143	125	250	173	0.302	125	100	0.3788	403	256	0.2632	17	15	0.8245	2.18
18	rd84_142	132	180	98	0.4308	124	111	0.2257	473	295	0.1904	119	78	0.4966	1.15
19	cnt3-5_180	215	556	653	0.0867	162	210	0.086	711	569	0.0718	36	31	0.7651	8.82
20	ham15_109	225	798	526	0.0304	188	304	0.0198	1010	607	0.0314	190	105	0.3531	11.25
21	ham15_108	579	1196	932	0.0305	552	667	0.0576	1853	1470	0.0387	173	99	0.3816	6.63
22	hwb_12	631	1556	1119	0.0699	602	699	0.0136	2262	1656	0.0055	193	100	0.361	5.16
23	misex1_241	1829	3821	2861	0.0068	1666	1971	0.0047	5146	3933	0.0046	12	12	0.8282	121.79
24	ham15_107	3442	6759	5355	0.0064	3158	3794	0.0075	9972	7543	0.0072	165	88	0.4045	53.93
25	dc2_222	4131	11327	9830	0.0029	3047	4582	0.0024	12355	10108	0.0026	8	8	0.8729	301.00
26	inc_237	4636	11134	16411	0.003	3348	4805	0.01	13697	11207	0.0035	32	22	0.7653	76.53
27	mlp4_245	16813	29521	23547	0.0035	14480	17234	0.002	41499	29239	0.0053	20	20	0.8052	151.92

In this study, the combined fidelity of the CNOT quantum circuit is simulated by Eq. 6. In order to verify the accuracy of the proposed fidelity calculation method, the fidelity calculated from the simulations is compared with the fidelity of the actual quantum hardware after implementation, and the results are shown in Fig. 11. Through the comparison of the fidelity of the 15 circuits in Table I, it is found that the simulated fidelity shows essentially the same fluctuations and trends as the actual fidelity, but the simulated fidelity is slightly higher than the actual fidelity. This phenomenon can be attributed to the existence of some specific noise and errors in the actual quantum hardware, such as crosstalk, measurement errors, and some other quality parameters of the qubits that may change over time. These factors aggravate the error rate and reduce the actual fidelity of the synthesized CNOT circuits. The experimental results demonstrate that the simulation method in this paper can predict the execution fidelity of the quantum circuit very well. Additionally, the fidelity predicted by the simulation method is in general agreement with the fidelity of the actual quantum hardware after execution. This demonstrates the reliability and validity of the simulation fidelity method.

In order to extend the CNOT circuit synthesis method to overcome its limitation of being applicable only to CNOT circuits, the Bernstein-Vazirani quantum algorithm is used as an example to illustrate the extensibility of the CNOT circuit synthesis method. Bernstein-Vazirani is a quantum algorithm containing some single quantum gates and CNOT gates, where the CNOT gates are continuous, as shown in Fig. 12. We synthesize this part of the CNOT circuits by using the LCNNS method, after adding the single quantum gates into the synthesized circuits, making them equivalent to the original circuits. This method was tested on different types of architectures, which are shown in Table III, containing 1-D, grid, and 2-D, as well as architectures with or without Hamiltonian paths. The experimental results, as depicted in Fig. 13, demonstrate that the LCNNS approach is applicable to a variety of architectures under NISQ. Furthermore, its applicability extends to circuits

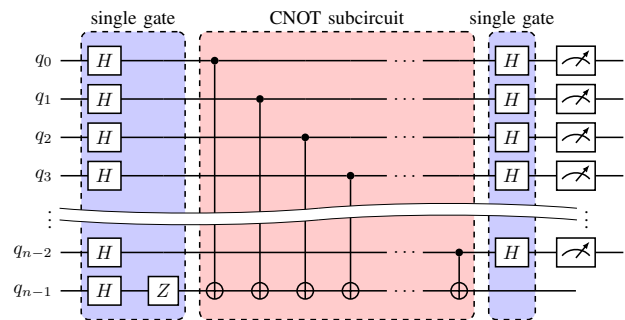


Fig. 12. Quantum circuit representation of the Bernstein-Vazirani algorithm.

TABLE III
PARAMETERS FOR DIFFERENT TYPES OF ARCHITECTURES

Architecture	Qubit	Layout	Include Hamiltonian paths
Manila	5	1-D	YES
Quito	5	2-D	NO
Jakarta	7	2-D	NO
Guadalupe	16	2-D	NO
Tokyo	20	Grid	YES
Almaden	20	Grid	NO
Kolkata	27	2-D	NO

including single quantum gates.

B. Results analysis

1) *CNOT count analysis*: The number of gates in a CNOT quantum circuit corresponds to the number of CNOT quantum gates used to manipulate and control the state of qubits. The number of CNOT gates is a critical metric for assessing the complexity of a CNOT quantum circuit, and it has a significant impact on the efficiency and reliability of quantum computing. A higher number of CNOT gates indicates more complex interactions between qubits, leading to longer execution times and higher error rates. Therefore, reducing the number of CNOT

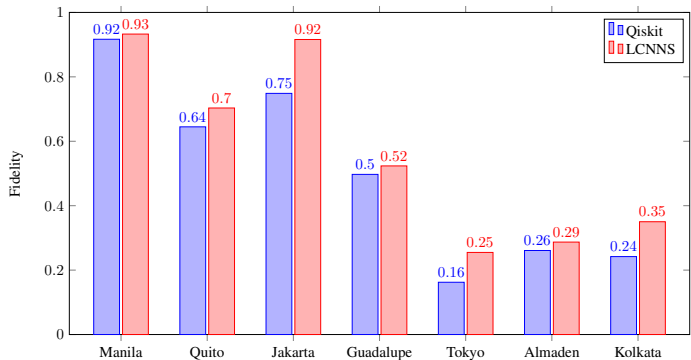


Fig. 13. Comparison of the fidelity of the Bernstein-Vazirani algorithm with Qiskit for each architecture in Table III.

gates after circuit transformation is essential for achieving efficient quantum computing. In contrast to the traditional way of inserting SWAP gates to achieve the NN of quantum gates, this paper achieves the NN synthesis of CNOT circuits by means of matrix transformation. This method enables the NN constraint of each gate in a CNOT circuit without inserting additional SWAP gates. As a result, it effectively reduces the number of CNOT gates in the circuit after the NN synthesis. Compared with Qiskit and HA, Tket further decomposes the CNOT gate and other gates into single quantum gates after the neighbors. So the number of CNOT gates in the Tket method is smaller than Qiskit and HA. As shown in Figs. 14(a) and 15(a), compared with the four NN methods and initial CNOT gates, the number of CNOT gates of proposed LCNNS method is lower, and the average optimization rate of the number of CNOT gates reaches 88.58%.

2) *Depth analysis*: Similar to the number of CNOT gates, the depth of CNOT quantum circuit is also an important indicator of the complexity and reliability of a CNOT quantum circuit. The depth of a CNOT quantum circuit refers to the number of layers of CNOT gates in a CNOT quantum circuit. Figures 14(b) and 15(b) show the comparison between the three methods and the LCNNS method in terms of circuit depth. From the Figs. 14(b) and 15(b), it can be seen that the circuit depth of the LCNNS method is much lower than those of the Qiskit, Tket and HA methods, with an average optimization rate of 90.70%. This is due to the significant effect of reducing the number of CNOT gates in the LCNNS method.

3) *Fidelity analysis*: The fidelity of a quantum circuit refers to the degree of similarity between the output result of the quantum circuit and the desired result, which can reflect the accuracy and reliability of the quantum circuit. In quantum computing, it is essential that the output result of a quantum circuit is as close as possible to the desired result, so fidelity is one of the important indicators of the performance of a quantum circuit. Figures 14(c) and 15(c) present a comparison between the Qiskit, Tket, HA and our LCNNS method in terms of circuit fidelity. It can be seen that the proposed LCNNS method greatly outperforms other methods in optimizing the circuit execution fidelity. In circuits within 1000 CNOT gates, the average fidelity is increased by 1.71 times. In circuits

containing over 1000 CNOT gates, the optimization effect is more pronounced. There are two reasons for this. On the one hand, the CNOT circuit synthesis method achieves quantum gates that satisfy NN constraint with as few CNOT gates as possible, and reducing the number of CNOT gates similarly reduces the source of double quantum gate errors, thus improving the fidelity of the synthesized CNOT circuit. On the other hand, the CNOT gates are prioritized to act on the path with a lower error rate during the matrix transformation, and the trade-off between the number of CNOT gates and the fidelity of the simulation is chosen to achieve the CNOT circuit synthesis at a lower cost.

Experiments demonstrate that the method in this paper achieves NN synthesis of CNOT quantum circuits with guaranteed quantum circuit fidelity. The fidelity of the experimental results in this paper are mostly greater than the 50% threshold, which is a better improvement compared with some circuits in Qiskit, Tket, and HA where the fidelity is below the 50% threshold. This achievement not only advances the latest in quantum circuit synthesis but also holds promise for practical quantum computation tasks.

VI. DISCUSSION

The method presented in this paper exhibits applicability across various IBM quantum computer architectures, especially those without Hamiltonian paths. Consequently, it can be effectively employed on a diverse range of quantum computing platforms in the NISQ. It is worth emphasizing that the suggested approach extends its utility to quantum circuits that incorporate not only pure CNOT gates but also additional single quantum gates, such as Clifford+T circuits. This versatility arises from the capability of reassembling a quantum circuit containing CNOT subcircuits into a form that satisfies the NN constraint. This is achieved by synthesizing the CNOT subcircuits and subsequently reassembling the circuit with single-qubit gates.

The implication of this is that CNOT circuits generated using our method can be readily scaled up for larger quantum computing architectures. There has been relevant research [28, 29] in this area, attempting to eliminate the limitations of CNOT circuit synthesis. In summary, the proposed NN synthesis method for CNOT circuits has the potential to substantially enhance the fidelity of CNOT circuits post NN synthesis and execution. This enhancement is of paramount significance for the practical deployment of CNOT circuits in various quantum computing contexts.

VII. CONCLUSION

This work presents an effective approach to synthesize CNOT quantum circuits on general quantum computing devices with and without Hamiltonian paths. Specifically, the proposed key-qubit priority model and tabu search algorithm are employed to dynamically adjust the mapping method of key qubits, with the aim of reducing the number of CNOT gates and increasing circuit fidelity after matrix transformation. Additionally, a noise-aware NN synthesis method based on layer convergence is presented. These approaches effectively

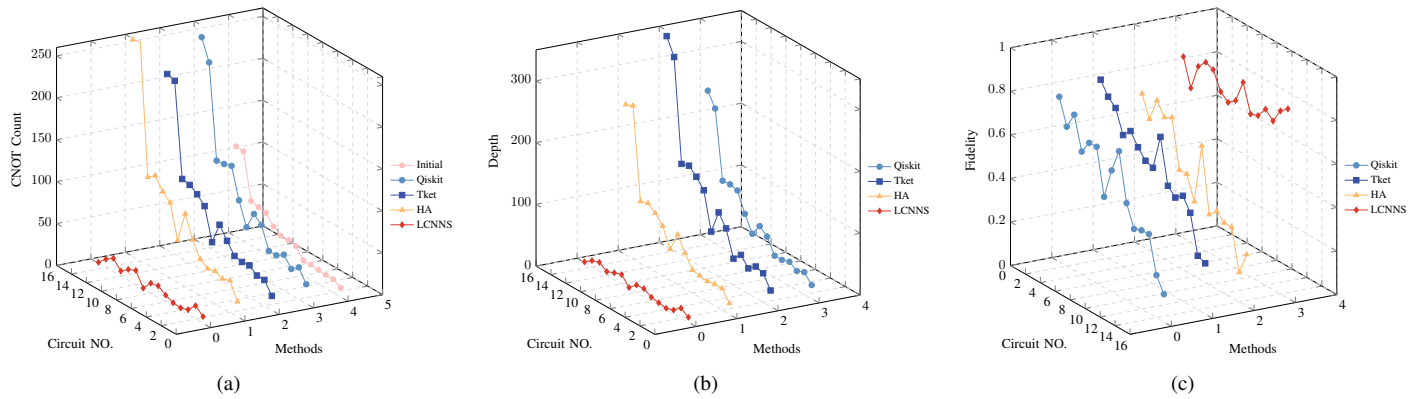


Fig. 14. Comparison of results in Table I under three performance indicators. (a) Comparison of CNOT gate numbers. (b) Comparison of depth. (c) Comparison of fidelity.

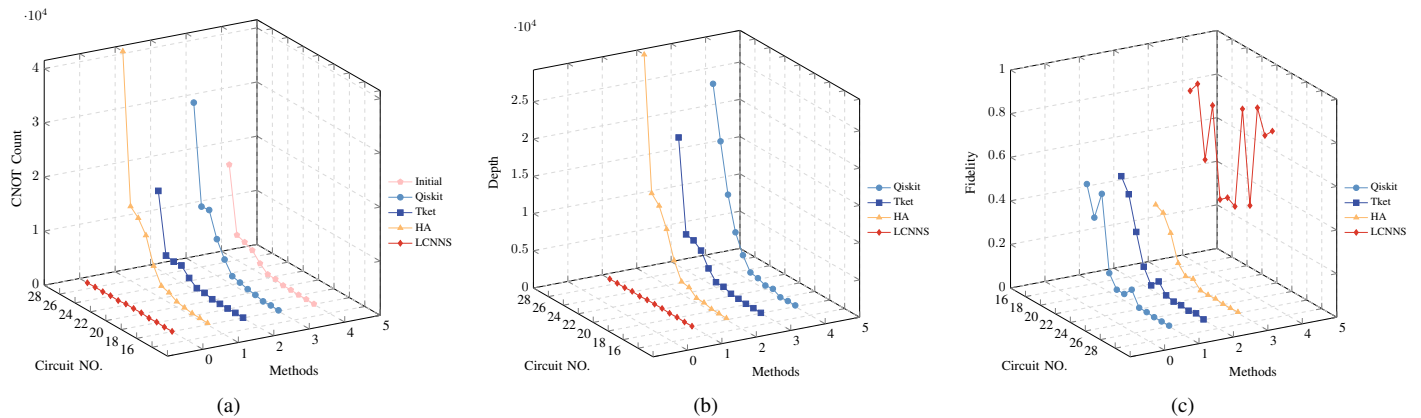


Fig. 15. Comparison of circuits in Table II under three performance indicators. (a) Comparison of CNOT gate numbers. (b) Comparison of depth. (c) Comparison of fidelity.

improve the fidelity of the synthesized circuit, providing a new solution to the problem of synthesizing CNOT circuits on real quantum computing devices. The experimental results, performed on the IBMQ_Quito quantum architecture in the IBMQ platform, demonstrate that the proposed method can significantly enhance the execution fidelity of CNOT quantum circuits on real quantum hardware. In future work, we will explore more efficient methods for circuit synthesis and optimization, and extend the NN synthesis of CNOT circuits to the synthesis of more complex quantum circuits.

ACKNOWLEDGMENT

The work was supported by the National Natural Science Foundation of China under Grant number 62072259, in part by the Natural Science Foundation of Jiangsu Province under Grant number BK20221411, in part by the PhD Start-up Fund of Nantong University under Grant number 23B03, in part by the Postgraduate Research and Practice Innovation Program of Jiangsu Province under Grant number SJCX21_1448 and SJCX23_1780.

REFERENCES

- [1] S. Juiang, K. A. Britt, A. J. McCaskey, T. S. Humble, and S. Kais, "Quantum annealing for prime factorization," *Scientific reports*, vol. 8, no. 1, p. 17667, 2018.
- [2] P. R. Giri and V. E. Korepin, "A review on quantum search algorithms," *Quantum Information Processing*, vol. 16, pp. 1–36, 2017.
- [3] S. Somaroo, C. Tseng, T. Havel, R. Laflamme, and D. G. Cory, "Quantum simulations on a quantum computer," *Physical review letters*, vol. 82, no. 26, p. 5381, 1999.
- [4] A. Kumar and S. Garhwal, "State-of-the-art survey of quantum cryptography," *Archives of Computational Methods in Engineering*, vol. 28, pp. 3831–3868, 2021.
- [5] H.-J. Werner, P. J. Knowles, G. Knizia, F. R. Manby, and M. Schütz, "Molpro: a general-purpose quantum chemistry program package," *Wiley Interdisciplinary Reviews: Computational Molecular Science*, vol. 2, no. 2, pp. 242–253, 2012.
- [6] V. Dunjko and H. J. Briegel, "Machine learning & artificial intelligence in the quantum domain: a review of recent progress," *Reports on Progress in Physics*, vol. 81, no. 7, p. 074001, 2018.
- [7] A. Barenco, C. H. Bennett, R. Cleve, D. P. DiVincenzo, N. Margolus, P. Shor, T. Sleator, J. A. Smolin, and H. Weinfurter, "Elementary gates for quantum computation," *Physical review A*, vol. 52, no. 5, p. 3457, 1995.
- [8] P. Zhu, X. Cheng, and Z. Guan, "An exact qubit allocation approach for nisq architectures," *Quantum Information Processing*, vol. 19, no. 11, p. 391, 2020.

- [9] X. Cheng, Z. Guan, and P. Zhu, “Nearest neighbor transformation of quantum circuits in 2d architecture,” *IEEE Access*, vol. 8, pp. 222 466–222 475, 2020.
- [10] P. Zhu, W. Ding, L. Wei, X. Cheng, Z. Guan, and S. Feng, “A variation-aware quantum circuit mapping approach based on multi-agent cooperation,” *IEEE Transactions on Computers*, 2023.
- [11] B. Nash, V. Gheorghiu, and M. Mosca, “Quantum circuit optimizations for nisq architectures,” *Quantum Science and Technology*, vol. 5, no. 2, p. 025010, 2020.
- [12] M. Amy, P. Azimzadeh, and M. Mosca, “On the controlled-not complexity of controlled-not–phase circuits,” *Quantum Science and Technology*, vol. 4, no. 1, p. 015002, 2018.
- [13] S. Zhang, J. Wu, and L. Li, “Characterization, synthesis, and optimization of quantum circuits over multiple-control z-rotation gates: A systematic study,” *Physical Review A*, vol. 108, no. 2, p. 022603, 2023.
- [14] X. Cheng, M. Zhu, X. Li, and Z. Guan, “Nearest neighbor synthesis of cnot circuit based on matrix transformation,” in *Advances in Natural Computation, Fuzzy Systems and Knowledge Discovery: Proceedings of the ICNC-FSKD 2021 17*. Springer, 2022, pp. 150–156.
- [15] K. Markov, I. Patel, and J. Hayes, “Optimal synthesis of linear reversible circuits,” *Quantum Information and Computation*, vol. 8, no. 3&4, pp. 0282–0294, 2008.
- [16] B. Schaeffer and M. Perkowski, “Linear reversible circuit synthesis in the linear nearest-neighbor model,” in *2012 IEEE 42nd International Symposium on Multiple-Valued Logic*. IEEE, 2012, pp. 157–160.
- [17] T. G. De Brugière, M. Baboulin, B. Valiron, S. Martiel, and C. Allouche, “Gaussian elimination versus greedy methods for the synthesis of linear reversible circuits,” *ACM Transactions on Quantum Computing*, vol. 2, no. 3, pp. 1–26, 2021.
- [18] A. Kissinger and A. Meijer-van de Griend, “Cnot circuit extraction for topologically-constrained quantum memories,” *Quantum Information and Computation*, vol. 20, pp. 581–596, 2020.
- [19] T. G. de Brugière, M. Baboulin, B. Valiron, S. Martiel, and C. Allouche, “Quantum cnot circuits synthesis for nisq architectures using the syndrome decoding problem,” in *Reversible Computation: 12th International Conference, RC 2020, Oslo, Norway, July 9-10, 2020, Proceedings 12*. Springer, 2020, pp. 189–205.
- [20] A. Meijer-van de Griend and S. M. Li, “Dynamic qubit allocation and routing for constrained topologies by cnot circuit re-synthesis,” in *Quantum Physics and Logic*. Electronic Proceedings in Theoretical Computer Science, 2022.
- [21] M. Zhu, X. Cheng, P. Zhu, L. Chen, and Z. Guan, “Physical constraint-aware cnot quantum circuit synthesis and optimization,” *Quantum Information Processing*, vol. 22, no. 1, p. 10, 2022.
- [22] C. Chen, B. Schmitt, H. Zhang, L. S. Bishop, and A. Javadi-Abhari, “Recursive methods for synthesizing permutations on limited-connectivity quantum computers,” *arXiv preprint arXiv:2207.06199*, 2022.
- [23] B. Wu, X. He, S. Yang, L. Shou, G. Tian, J. Zhang, and X. Sun, “Optimization of cnot circuits on limited-connectivity architecture,” *Physical Review Research*, vol. 5, no. 1, p. 013065, 2023.
- [24] C.-K. Li, R. Roberts, and X. Yin, “Decomposition of unitary matrices and quantum gates,” *International Journal of Quantum Information*, vol. 11, no. 01, p. 1350015, 2013.
- [25] S. Niu, A. Suau, G. Staffelbach, and A. Todri-Sanial, “A hardware-aware heuristic for the qubit mapping problem in the nisq era,” *IEEE Transactions on Quantum Engineering*, vol. 1, pp. 1–14, 2020.
- [26] S. B. Nadler Jr, “Continuum theory and graph theory: disconnection numbers,” *Journal of the London Mathematical Society*, vol. 2, no. 1, pp. 167–181, 1993.
- [27] U. Brandes, “A faster algorithm for betweenness centrality,” *Journal of mathematical sociology*, vol. 25, no. 2, pp. 163–177, 2001.
- [28] V. Gheorghiu, J. Huang, S. M. Li, M. Mosca, and P. Mukhopadhyay, “Reducing the cnot count for clifford+t circuits on nisq architectures,” *IEEE Transactions on Computer-Aided Design of Integrated Circuits and Systems*, 2022.
- [29] S. Zhang, K. Huang, and L. Li, “Automatic depth-optimized quantum circuit synthesis for diagonal unitary matrices with asymptotically optimal gate count,” *arXiv preprint arXiv:2212.01002*, 2022.